Crystal structures and enhancement of photoluminescence intensities by effective doping for lithium tantalate phosphors

Hiroaki Ichioka,[1] Shohei Furuya,[2] Toru Asaka,[1] Hiromi Nakano,[2] and Koichiro Fukuda[1,a)]
[1]*Department of Materials Science and Engineering, Nagoya Institute of Technology, Nagoya 466-8555, Japan*
[2]*Department of Environmental and Life Sciences, Toyohashi University of Technology, Toyohashi 441-8580, Japan*

(Received 14 April 2015; accepted 10 July 2015)

Crystal structures of $(Li_{0.925}Eu^{3+}_{0.025})TaO_3$, $(Li_{0.968}Eu^{3+}_{0.032})(Ta_{0.81}Ti_{0.19})O_{2.937}$, $(Li_{0.967}Sm^{3+}_{0.033})(Ta_{0.89}Ti_{0.11})O_{2.978}$, and $(Li_{0.950}Sm^{3+}_{0.033}Mg_{0.017})(Ta_{0.89}Ti_{0.11})O_{2.987}$ were investigated by X-ray powder diffraction. The initial structural parameters, taken from those of the isomorphous compound $(Li_{0.977}Eu^{3+}_{0.023})(Ta_{0.89}Ti_{0.11})O_{2.968}$ (space group $R3c$ and $Z = 6$), were refined by the Rietveld method. A pattern-fitting method based on the maximum-entropy method was subsequently used to determine the three-dimensional electron-density distributions (EDDs) that are free from the structural bias. We confirmed that the EDDs are in accord with the resulting structural models, each of which was composed of the [(Ta, Ti)O_6] octahedron and [(Li, Eu, Sm, Mg)O_{12}] polyhedron. We compared these polyhedra and found that the prominent difference among these compounds was the centroid-to-(Li, Eu, Sm, Mg) distance (eccentricity) of [(Li, Eu, Sm, Mg)O_{12}]. The high correlation was demonstrated between the magnitude of eccentricity and photoluminescence intensity under near ultraviolet excitation. © *2015 International Centre for Diffraction Data.*
[doi:10.1017/S0885715615000688]

Key words: doped lithium tantalate, X-ray powder diffraction, Rietveld method, electron-density distributions, phosphors

I. INTRODUCTION

Recently, $Li(Ta_{1-x}Ti_x)O_{3-x/2}$ crystals ($0 \le x \le 0.25$), when they are activated with rare-earth ions (= Sm^{3+}, Eu^{3+}, Er^{3+}, Dy^{3+}, and/or Tm^{3+}), have been found to demonstrate the highly efficient emission with various colors upon near ultraviolet (UV) excitation (Nakano *et al.*, 2012, 2013). Nakano *et al.* (2012) have investigated the photoluminescence (PL) properties of the Eu^{3+}-doped $Li(Ta_{1-x}Ti_x)O_{3-x/2}$ phosphors and found that their PL intensities have been dependent on the x-value. The intensity was the highest for phosphor with $x = 0.11$. The phosphors with x-values lower or higher than this value thus showed the inferior intensities. Uchida *et al.* (2013) used the X-ray powder diffraction (XRPD) method to determine the crystal structure of $Li(Ta_{1-x}Ti_x)O_{3-x/2}$:$Eu^{3+}$ phosphor with $x = 0.11$ (space group $R3c$), the chemical formula of which is $(Li_{0.977}Eu^{3+}_{0.023})(Ta_{0.89}Ti_{0.11})O_{2.968}$. They found that it is isostructural with $LiTaO_3$ (Hsu, *et al.*, 1997), in which both (Li, Eu) and (Ta, Ti) sites are located on the triad axis (Figure 1). The (Li, Eu) atom is 12-fold coordinated by oxygen and (Ta, Ti) site is coordinated with six oxygen atoms. The (Li, Eu) site is relatively largely displaced from the centroid of [(Li, Eu)O_{12}] polyhedra in the [00$\bar{1}$] direction by 0.047 nm, in contrast to the (Ta, Ti) site located nearly at the centroid of the [(Ta, Ti)O_6] octahedra (Uchida *et al.*, 2013). To clarify the mechanism of high efficiency and further improve the PL performance of doped lithium tantalate phosphors, it is necessary to obtain the structural

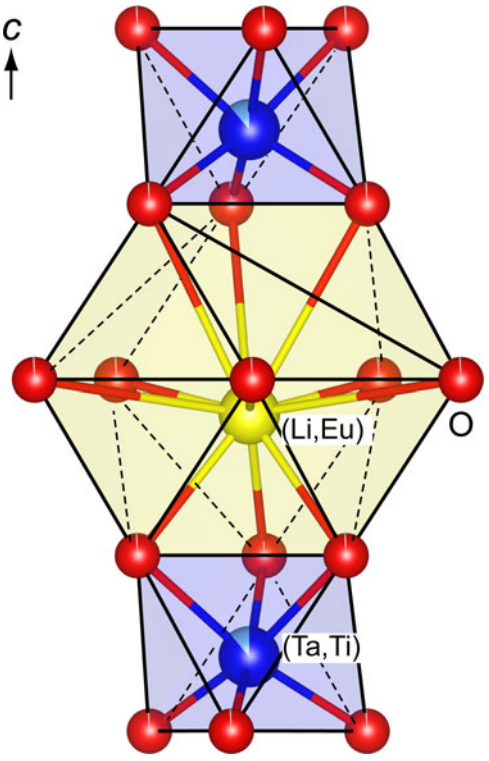

Figure 1. (Color online) Part of the crystal structure of $(Li_{0.977}Eu^{3+}_{0.023})(Ta_{0.89}Ti_{0.11})O_{2.968}$ viewed along [110], showing coordination polyhedra for (Li, Eu) and (Ta, Ti). Because the occupancy of the oxygen site is less than unity, the O atoms are depicted as red circle graphs for occupancies. Blue and cyan bicolor balls are for Ta (blue) and Ti (cyan) sites. Yellow and magenta bicolor balls are for Li (yellow) and Eu (magenta) sites. Structural parameters are determined by Uchida *et al.* (2013).

a)Author to whom correspondence should be addressed. Electronic mail: fukuda.koichiro@nitech.ac.jp

TABLE I. Phase composition (mol%).

Sample	Doped lithium tantalate	$EuTaO_4$	$Li_4Ti_5O_{12}$	Li_3TaO_4	Total
LETO	99.90	0.10	–	–	100
LETTO	94.61	–	1.65	3.74	100
LSTTO	96.73	–	–	3.27	100
LSMTTO	96.74	–	–	3.26	100

TABLE II. Crystal data for $(Li_{0.925}Eu^{3+}{}_{0.025})TaO_3$.

Chemical formula	$(Li_{0.925}Eu^{3+}{}_{0.025})TaO_3$
Space group	*R*3*c* (No. 161)
a/nm	0.515 741(2)
c/nm	1.377 230(4)
V/nm^3	0.317 249(1)
Z	6
D_x/Mg m^{-3}	7.511

information especially on the coordination environment of the rare-earth ions.

We reported in our previous study the crystal structure of $(Li_{0.977}Eu^{3+}{}_{0.023})(Ta_{0.89}Ti_{0.11})O_{2.968}$ (Uchida *et al.*, 2013), the (Li, Eu) site position which was displayed clearly from three-dimensional (3D) electron-density distributions (EDDs). We used the recent analytical techniques for crystal-structure analysis from XRPD data, which includes combined use of the Rietveld method (Rietveld, 1967), the maximum-entropy method (MEM) (Takata *et al.*, 2001) and the MEM-based pattern fitting (MPF) method (Momma *et al.*, 2013). As the result of the alternately repeated MEM and MPF analyses (REMEDY cycle), we are able to visualize the EDDs that are free from the bias toward the structural models (Izumi *et al.*, 2001). Thus, the structural details can be seen clearly from the EDDs.

In the present study, we prepared four types of doped lithium tantalate phosphors; they are $Li(Ta_{1-x}Ti_x)O_{3-x/2}:Eu^{3+}$ with $x = 0$ and $x = 0.19$ and $(Li_{1-y}Mg_y)(Ta_{0.89}Ti_{0.11})O_{2.945+y/2}:Sm^{3+}$ with $y = 0$ and $y = 0.017$. We determined these crystal structures and compared their structural details together with those of $(Li_{0.977}Eu^{3+}{}_{0.023})(Ta_{0.89}Ti_{0.11})O_{2.968}$ ($x = 0.11$). The *z* coordinates of the (Li, Eu) and (Li, Sm, Mg) sites were markedly different among the isomorphous structures. Hence, we discuss the close relationship between the PL intensity and the coordination environment of these sites.

II. EXPERIMENTAL

A. Syntheses

We prepared four types of powder specimens with different starting compositions of [Li:Eu:Ta] = [0.965:0.035:1] (sample LETO), [Li:Eu:Ta:Ti] = [0.974:0.026:0.75:0.25] (sample LETTO), [Li:Sm:Ta:Ti] = [0.969:0.031:0.89:0.11] (sample LSTTO), and [Li:Sm:Mg:Ta:Ti] = [0.954:0.030:0.016:0.89:0.11] (sample LSMTTO) in atomic ratio from the chemicals of Li_2CO_3, Eu_2O_3, Sm_2O_3, MgO, Ta_2O_5, and TiO_2. Each of the well-mixed chemicals was heated at 1273 K for 3 h, and then successively at 1423 K for 24 h (samples LETO and LETTO) and for 15 h (samples LSTTO and LSMTTO), and finally cooled to ambient temperature. We finely ground the densely sintered pellets and obtained the fine powder specimens suitable for XRPD. The former two samples (LETO and LSTTO) were prepared under exactly the same experimental conditions as those of $Li(Ta_{1-x}Ti_x)O_{3-x/2}:Eu^{3+}$ phosphors examined for PL properties in a previous study (Nakano *et al.*, 2012).

B. Characterization

The XRPD intensities in the 2θ range of 10.0°–149.0° ($CuK\alpha_1$) with 15 559 total data points were collected on a diffractometer in the Bragg–Brentano geometry (X'Pert PRO Alpha-1, PANalytical B.V., Almelo, The Netherlands). The X-ray generator was operated at 45 kV and 40 mA. We used a computer program VESTA (Momma and Izumi, 2011) to visualize the structural models, equidensity isosurfaces of EDDs and 2D EDD maps. Distortion parameters for the coordination polyhedra were determined using a computer program IVTON (Balic-Zunic and Vickovic, 1996). Excitation and emission spectra were obtained for the $(Li_{1-y}Mg_y)(Ta_{0.89}Ti_{0.11})O_{2.945+y/2}:Sm^{3+}$ phosphors by a PL spectrometer (model FP-6500, JASCO International Co., Ltd., Tokyo, Japan). We measured the PL intensities on the sintered sample surface to eliminate the effects of powder particle size and degree of crystallinity.

III. RESULTS AND DISCUSSION

A. Crystal structure refinements and electron-density distributions

The sample LETO was composed of both Eu^{3+}-doped lithium tantalate and a small amount of $EuTaO_4$ (Krylov and Strelina, 1963). We successfully indexed the XRPD peaks, corresponding to the doped lithium tantalate, with a hexagonal unit cell. Initial structural parameters were taken from those of $(Li_{0.977}Eu^{3+}{}_{0.023})(Ta_{0.89}Ti_{0.11})O_{2.968}$ (space group *R*3*c*) determined by Uchida *et al.* (2013). There is one (Li, Eu) site and one Ta site, both of which are located at the Wyckoff position 6*a*, and one O site at 18*b* in the hexagonal unit cell ($Z = 6$). We refined the structural parameters of all atoms using the Rietveld method on a computer program RIETAN-FP (Izumi and Momma, 2007). We quantitatively determined the phase composition of the sample using the phase-analysis method based on Brindley's procedure

TABLE III. Structural parameters and isotropic atomic displacement parameters ($100 \times B$/nm^2) for $(Li_{0.925}Eu^{3+}{}_{0.025})TaO_3$.

Site position	Wyckoff	*g*	*x*	*y*	*z*	$100 \times B$/nm^2
(Li,Eu)	6*a*	0.925/0.025	0	0	0.2795(5)	1.3
Ta	6*a*	1.0	0	0	0	0.40(5)
O	18*b*	1.0	0.0450(10)	0.3243(14)	0.0969(3)	0.52(8)

https://doi.org/10.1017/S0885715615000688 Published online by Cambridge University Press

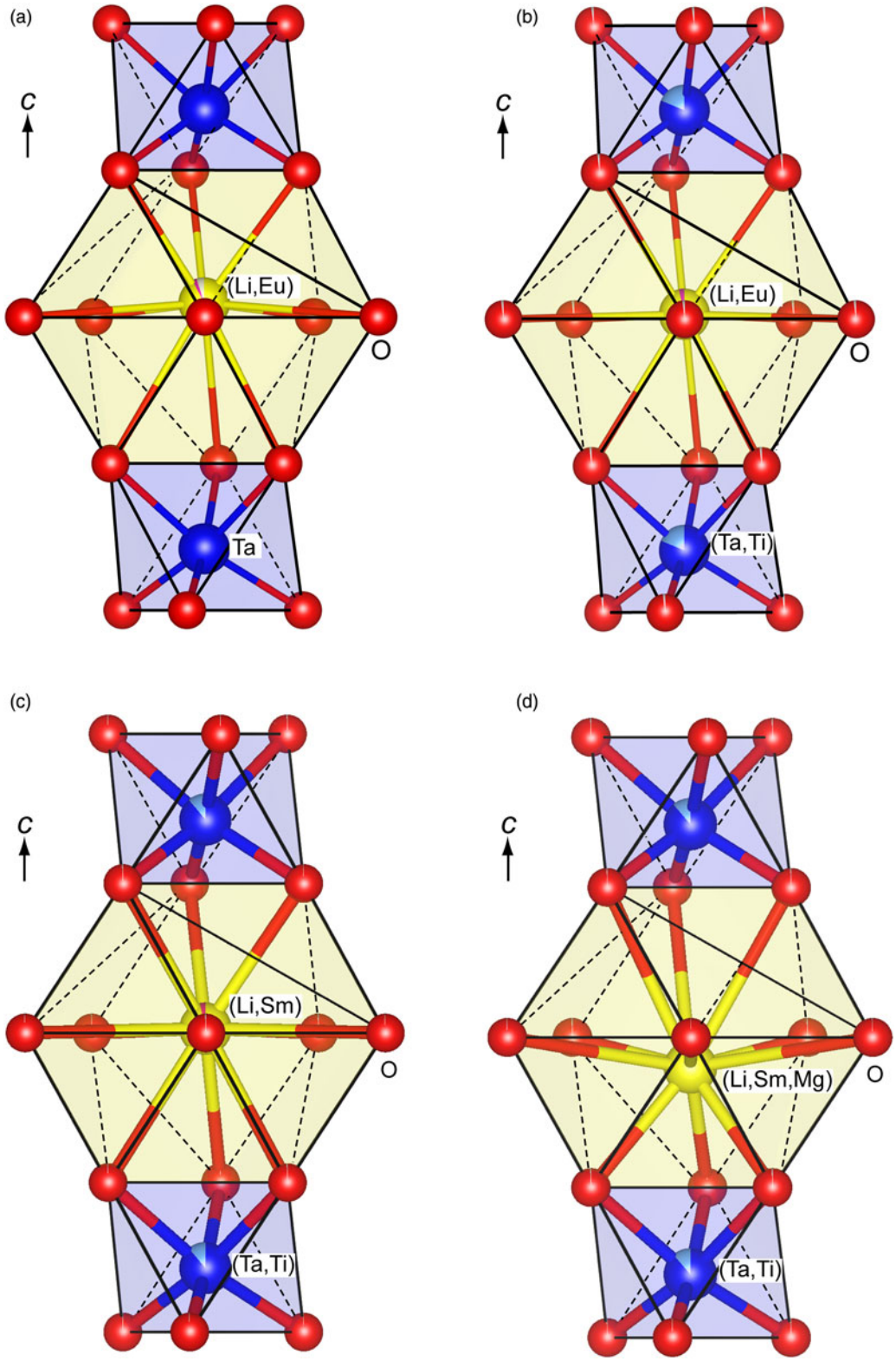

Figure 2. (Color online) (a) Part of the crystal structure viewed along [110] of $(Li_{0.925}Eu^{3+}_{0.025})TaO_3$ in sample LETO. Yellow and magenta bicolor balls are for Li (yellow) and Eu (magenta) sites. Blue balls are for Ta sites. (b) Part of the crystal structure viewed along [110] of $(Li_{0.968}Eu^{3+}_{0.032})(Ta_{0.81}Ti_{0.19})O_{2.937}$ in sample LETTO. Yellow and magenta bicolor balls are for Li (yellow) and Eu (magenta) sites. Because the occupancy of the oxygen site is less than unity, the O atoms are depicted as red circle graphs for occupancies. Blue and cyan bicolor balls are for Ta (blue) and Ti (cyan) sites. (c) Part of the crystal structure viewed along [110] of $(Li_{0.967}Sm^{3+}_{0.033})(Ta_{0.89}Ti_{0.11})O_{2.978}$ in sample LSTTO. Yellow and magenta bicolor balls are for Li (yellow) and Sm (magenta) sites. Because the occupancy of the oxygen site is less than unity, the O atoms are depicted as red circle graphs for occupancies. Blue and cyan bicolor balls are for Ta (blue) and Ti (cyan) sites. (d) Part of the crystal structure viewed along [110] of $(Li_{0.950}Sm^{3+}_{0.033}Mg_{0.017})(Ta_{0.89}Ti_{0.11})O_{2.987}$ in sample LSMTTO. Yellow and magenta bicolor balls are for Li (yellow) and (Sm, Mg) (magenta) sites. Because the occupancy of the oxygen site is less than unity, the O atoms are depicted as red circle graphs for occupancies. Blue and cyan bicolor balls are for Ta (blue) and Ti (cyan) sites.

https://doi.org/10.1017/S0885715615000688 Published online by Cambridge University Press

TABLE IV. Crystal data for $(Li_{0.968}Eu^{3+}_{0.032})(Ta_{0.81}Ti_{0.19})O_{2.937}$.

Chemical formula	$(Li_{0.968}Eu^{3+}_{0.032})(Ta_{0.81}Ti_{0.19})O_{2.937}$
Space group	*R*3*c* (No. 161)
a/nm	0.518 222(3)
c/nm	1.372 199(7)
V/nm^3	0.319 139(3)
Z	6
D_x/Mg m^{-3}	6.688

TABLE V. Crystal data for $(Li_{0.967}Sm^{3+}_{0.033})(Ta_{0.89}Ti_{0.11})O_{2.978}$.

Chemical formula	$(Li_{0.967}Sm^{3+}_{0.033})(Ta_{0.89}Ti_{0.11})O_{2.978}$
Space group	*R*3*c* (No. 161)
a/nm	0.517 857(3)
c/nm	1.373 060(6)
V/nm^3	0.318 889(3)
Z	6
D_x/Mg m^{-3}	7.050

TABLE VI. Crystal data for $(Li_{0.950}Sm^{3+}_{0.033}Mg_{0.017})(Ta_{0.89}Ti_{0.11})O_{2.987}$.

Chemical formula	$(Li_{0.950}Sm^{3+}_{0.033}Mg_{0.017})(Ta_{0.89}Ti_{0.11})O_{2.987}$
Space group	*R*3*c* (No. 161)
a/nm	0.517 517(3)
c/nm	1.373 688(7)
V/nm^3	0.318 616(3)
Z	6
D_x/Mg m^{-3}	7.070

(Brindley, 1945), the subroutine of which was implemented in the program RIETAN-FP. The phase composition was, under the condition of effective particle radii being 5.00 μm, found to be 99.90 mol% Eu^{3+}-doped lithium tantalate and 0.10 mol% $EuTaO_4$ (Table I). We determined the chemical formula of the former by subtracting the $EuTaO_4$ component from the bulk chemical composition. Because the bulk atomic ratio of sample LETO was [Li:Eu:Ta] = [0.965:0.035:1], the chemical formula should be $(Li_{0.925}Eu^{3+}_{0.025})TaO_3$ ($x = 0$). The Rietveld refinement result was satisfactory due to the relatively low reliability (*R*) indices (Young, 1993) of R_{wp} = 10.14%, $S(=R_{wp}/R_e) = 1.29\%$, $R_p = 7.24\%$, $R_B = 2.84\%$, and $R_F = 1.40\%$. We summarized the crystal data in Table II, and the final atomic positional parameters and isotropic atomic displacement parameters (ADPs) in Table III, where the figures in parentheses of these tables indicate estimated standard uncertainties.

We visualized the 3D EDDs with 108 × 108 × 276 voxels in the unit cell, the spatial resolution of which is ~0.005 nm, using the MPF method on the computer programs Dysnomia (Momma *et al.*, 2013) and RIETAN-FP to confirm the validity of the structural model (Figure S1(a) in Supplemental Data). The one REMEDY cycle further decreased the R_B- and R_F-indices to 1.63 and 0.80%, respectively ($R_{wp} = 10.00\%$, $S = 1.27$, and $R_p = 6.89\%$). The reduction of these *R*-indices, which must be induced by slight improvements of EDDs, implies that the EDDs more clearly demonstrate the structural details as compared with the ball-and-stick model in Figure 2(a). The XRPD patterns that are obtained by observation and calculation for the final MPF, together with their difference, are plotted in Figure S2(a) (see Supplemental Data).

The other samples of LETTO, LSTTO, and LSMTTO were composed of doped lithium titanotantalate and small amounts of impurities of Li_3TaO_4 (Agulyanskii *et al.*, 1986) and/or $Li_4Ti_5O_{12}$ (Leonidov *et al.*, 2003). The analytical processes for these samples were very similar to that of LETO aforementioned. We determined the phase compositions (Table I) and subsequently determined the chemical formulae of doped lithium titanotantalate compounds from calculation by subtracting the impurity components from the bulk chemical compositions. We obtained the satisfactory *R* indices for

TABLE VII. Structural parameters and isotropic atomic displacement parameters ($100 \times B$/nm^2) for $(Li_{0.968}Eu^{3+}_{0.032})(Ta_{0.81}Ti_{0.19})O_{2.937}$.

Site position	Wyckoff	*g*	*x*	*y*	*z*	$100 \times B$/nm^2
(Li,Eu)	6*a*	0.968/0.032	0	0	0.2684(5)	0.8(1)
(Ta,Ti)	6*a*	0.81/0.19	0	0	0	0.19(3)
O	18*b*	0.979	0.0439(11)	0.3201(17)	0.0960(4)	0.48(6)

TABLE VIII. Structural parameters and isotropic atomic displacement parameters ($100 \times B$/nm^2) for $(Li_{0.967}Sm^{3+}_{0.033})(Ta_{0.89}Ti_{0.11})O_{2.978}$.

Site position	Wyckoff	*g*	*x*	*y*	*z*	$100 \times B$/nm^2
(Li,Sm)	6*a*	0.967/0.033	0	0	0.2671(4)	0.9(1)
(Ta,Ti)	6*a*	0.89/0.11	0	0	0	0.54(4)
O	18*b*	0.993	0.0520(14)	0.3216(22)	0.0955(5)	0.87(8)

TABLE IX. Structural parameters and isotropic atomic displacement parameters ($100 \times B$/nm^2) for $(Li_{0.950}Sm^{3+}_{0.033}Mg_{0.017})(Ta_{0.89}Ti_{0.11})O_{2.987}$.

Site position	Wyckoff	*g*	*x*	*y*	*z*	$100 \times B$/nm^2
(Li,Sm,Mg)	6*a*	0.950/0.033/0.017	0	0	0.2291(5)	1.2(1)
(Ta,Ti)	6*a*	0.89/0.11	0	0	0	0.54(8)
O	18*b*	0.996	0.0604(15)	0.323 52(23)	0.0961(4)	0.7(1)

https://doi.org/10.1017/S0885715615000688 Published online by Cambridge University Press

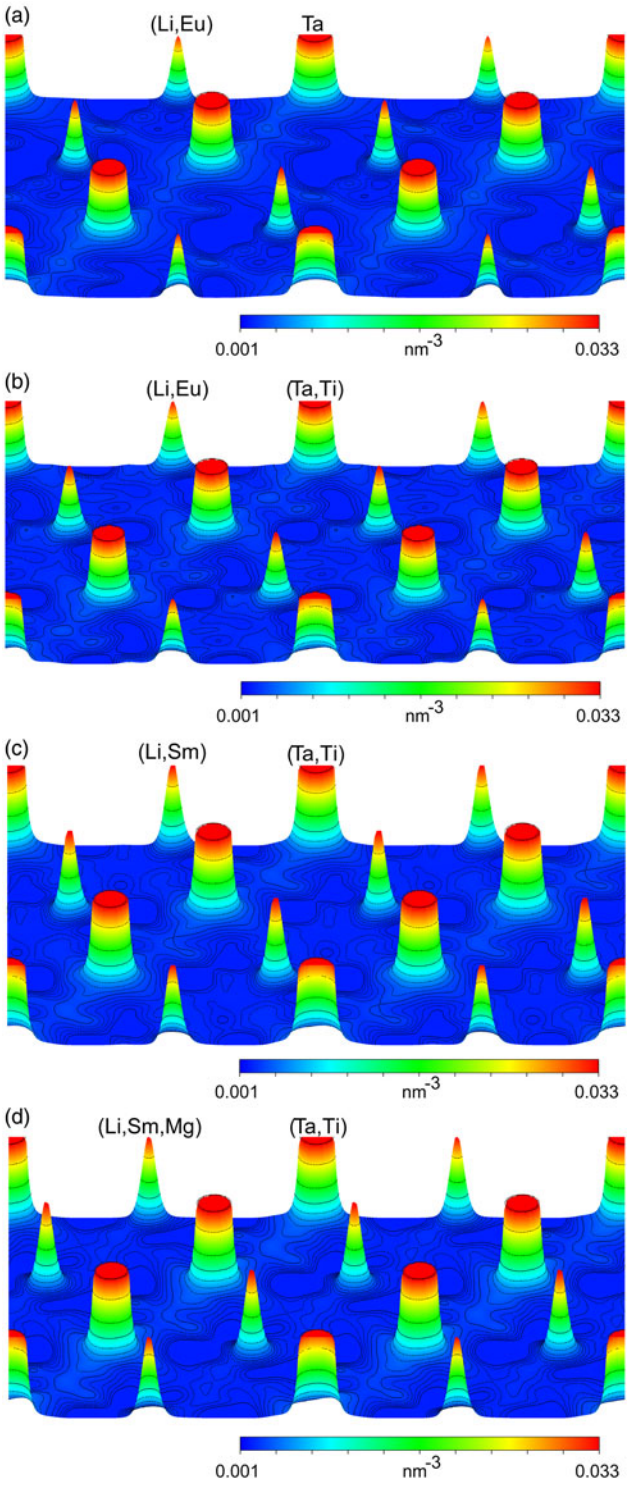

Figure 3. (Color online) (a) Bird's eye view of electron densities determined by MPF of the (Li, Eu) and Ta atoms on the (110) plane of $(Li_{0.925}Eu^{3+}_{0.025})TaO_3$ in sample LETO. (b) Bird's eye view of electron densities determined by MPF of the (Li, Eu) and (Ta, Ti) atoms on the (110) plane of $(Li_{0.968}Eu^{3+}_{0.032})(Ta_{0.81}Ti_{0.19})O_{2.937}$ in sample LETTO. (c) Bird's eye view of electron densities determined by MPF of the (Li, Sm) and (Ta, Ti) atoms on the (110) plane of $(Li_{0.967}Sm^{3+}_{0.033})(Ta_{0.89}Ti_{0.11})O_{2.978}$ in sample LSTTO. (d) Bird's eye view of electron densities determined by MPF of the (Li, Sm, Mg) and (Ta, Ti) atoms on the (110) plane of $(Li_{0.950}Sm^{3+}_{0.033}Mg_{0.017})(Ta_{0.89}Ti_{0.11})O_{2.987}$ in sample LSMTTO.

all of the Rietveld refinements (Table SI in Supplemental Data), the refined structural models of which are shown in Figures S1(b)–S1(d) (see Supplemental Data). The crystal data of doped lithium titanotantalate compounds are given in Tables IV, V and VI, and the final atomic positional parameters and isotropic ADPs are given in Tables VII, VIII and IX, where the figures in parentheses of these tables indicate estimated standard uncertainties. We applied the MPF method and further decreased the R indices after two REMEDY cycles (Table SI in Supplemental Data). Observed, calculated, and difference XRPD patterns for the final MPF are plotted in Figures S2(b)–S2(d) (see Supplemental Data).

Figures 2(a)–2(d) show parts of the refined crystal structures of doped lithium tantalate phosphors, the chemical formulas of which are $(Li_{0.925}Eu^{3+}_{0.025})TaO_3$ ($x = 0$) in sample LETO, $(Li_{0.968}Eu^{3+}_{0.032})(Ta_{0.81}Ti_{0.19})O_{2.937}$ ($x = 0.19$) in sample LETTO, $(Li_{0.967}Sm^{3+}_{0.033})(Ta_{0.89}Ti_{0.11})O_{2.978}$ ($y = 0$) in sample LSTTO, and $(Li_{0.950}Sm^{3+}_{0.033}Mg_{0.017})(Ta_{0.89}Ti_{0.11})O_{2.987}$ ($y = 0.017$) in sample LSMTTO. We confirmed that all of them are isostructural with $(Li_{0.977}Eu^{3+}_{0.023})(Ta_{0.89}Ti_{0.11})O_{2.968}$ ($x = 0.11$) (Uchida *et al.*, 2013). The individual equidensity isosurfaces of 3D EDDs were in accord with the arrangements of atoms. The 2D EDD maps show that the positions of (Li, Eu, Sm, Mg) and (Ta, Ti) sites are successfully disclosed by the EDDs (Figure 3). The EDD voxel data have several local maximum, which correspond to the coordinates of atoms. We determined the amounts of deviations between the maxima positions and corresponding atomic coordinates to find that they were necessarily less than 0.003 nm, which is within the resolution limit of the 3D EDDs. Thus, we concluded that the refined structural models would satisfactorily represent the corresponding crystal structures.

B. Structure comparison and photoluminescence property

The coordination elements of each structure are the [(Ta, Ti)O_6] octahedron and [(Li, Eu, Sm, Mg)O_{12}] polyhedron. Selected interatomic distances and their standard deviations are listed in Tables SII–SV (see Supplemental Data). In comparing the polyhedral distortion parameters of [(Ta, Ti)O_6] octahedra (Table X) among the four isomorphous structures, together with those of $(Li_{0.977}Eu^{3+}_{0.023})(Ta_{0.89}Ti_{0.11})O_{2.968}$ (Uchida *et al.*, 2013), we found that the V_S/V_P-values (i.e., the ratios of the volumes of the circumscribed sphere and the polyhedron) ranged between 3.129 and 3.157, and hence they were close to the relevant value of regular octahedron ($= 3.1416$) (Makovicky and Balic-Zunic, 1998). Thus, the [(Ta, Ti)O_6] polyhedra were only slightly distorted from the regular octahedra. The values for distortion parameters (Δ r_S, V_S, σ, and V_P) were almost the same among the five phosphors, hence we concluded that the [(Ta, Ti)O_6] octahedra were all comparable with one another. With [(Li, Eu, Sm, Mg)O_{12}] polyhedra, the centroid-to-(Li, Eu, Sm, Mg) distances (Δ-values) widely varied from 0.004 to 0.047 among the five compounds, although the other polyhedral parameter values (r_S, V_S, σ, and V_P) were almost unchanged (Table X).

Here, we compare the eccentricity vectors $\boldsymbol{\Delta}$, which are defined from the centroids to the (Li, Eu, Sm, Mg) sites of the [(Li, Eu, Sm, Mg)O_{12}] polyhedra, to indicate more clearly the features of the crystal structures of $Li(Ta_{1-x}Ti_x)O_{3-x/2}:Eu^{3+}$ and $(Li_{1-y}Mg_y)(Ta_{0.89}Ti_{0.11})O_{2.945+y/2}:Sm^{3+}$ by the directions of $\boldsymbol{\Delta}$ as well as their magnitudes $|\boldsymbol{\Delta}|$ (Uchida *et al.*, 2013). With $(Li_{0.977}Eu^{3+}_{0.023})(Ta_{0.89}Ti_{0.11})O_{2.968}$ ($x = 0.11$)

https://doi.org/10.1017/S0885715615000688 Published online by Cambridge University Press

TABLE X. Polyhedral distortion parameters.

Compound	Polyhedron	Δ/nm	r_S/nm	V_S/nm^3	σ	V_P/nm^3	V_S/V_P
$(Li_{0.925}Eu^{3+}_{0.025})TaO_3$	$[(Li,Eu)O_{12}]$	0.019	0.269	0.0971	0.821	0.0428	2.269
	$[TaO_6]$	0.014	0.198	0.0323	1	0.0103	3.136
$(Li_{0.968}Eu^{3+}_{0.032})(Ta_{0.81}Ti_{0.19})O_{2.937}$	$[(Li,Eu)O_{12}]$	0.004	0.270	0.0974	0.830	0.0431	2.260
	$[(Ta,Ti)O_6]$	0.010	0.198	0.0325	1	0.0103	3.155
$(Li_{0.977}Eu^{3+}_{0.023})(Ta_{0.89}Ti_{0.11})O^{*}_{2.968}$	$[(Li,Eu)O_{12}]$	0.047	0.270	0.0981	0.826	0.0429	2.287
	$[(Ta,Ti)O_6]$	0.012	0.198	0.0326	1	0.0104	3.135
$(Li_{0.967}Sm^{3+}_{0.033})(Ta_{0.89}Ti_{0.11})O_{2.978}$	$[(Li,Sm)O_{12}]$	0.006	0.269	0.0965	0.833	0.0429	2.249
	$[(Ta,Ti)O_6]$	0.016	0.197	0.0322	1	0.0102	3.157
$(Li_{0.950}Sm^{3+}_{0.033}Mg_{0.017})(Ta_{0.89}Ti_{0.11})O_{2.987}$	$[(Li,Sm,Mg)O_{12}]$	0.046	0.269	0.0945	0.843	0.0431	2.193
	$[(Ta,Ti)O_6]$	0.019	0.196	0.0316	1	0.0101	3.129

Δ, centroid-to-cation distance (eccentricity); r_S, radius of sphere fitted to ligands; V_S, sphere volume; σ, sphericity; V_P, volume of coordination polyhedron. For explanation, see Makovicky and Balic-Zunic (1998).

* Structural parameters by Uchida *et al.* (2013).

(Figure 1), the eccentricity vector $\boldsymbol{\Delta}$ is in the $[00\bar{1}]$ direction and $|\boldsymbol{\Delta}| = 0.047$ nm. On the other hand, the $\boldsymbol{\Delta}$ vectors for $(Li_{0.925}Eu^{3+}_{0.025})TaO_3$ ($x = 0$) (Figure 2(a)) and $(Li_{0.968}Eu^{3+}_{0.032})(Ta_{0.81}Ti_{0.19})O_{2.937}$ ($x = 0.19$) (Figure 2(b)) are in the [001] direction with the smaller magnitudes of 0.019 and 0.004 nm, respectively. Thus, the marked difference among the three phosphors was clarified as the degree of eccentricity along the *c*-axis of the (Li, Eu) position in [(Li, Eu)O_{12}]. Because the concentrations of Eu in the (Li, Eu) sites are relatively low and nearly the same among the three compounds with $x = 0$, 0.11, and 0.19, the replacement of Ti for Ta would mainly induce the displacement of the (Li, Eu) site along the *c*-axis, without changing the outer shapes of both [(Li, Eu)O_{12}] and [(Ta, Ti)O_6] polyhedra. The PL intensities determined by Nakano *et al.* (2012) were highest for the Li$(Ta_{1-x}Ti_x)O_{3-x/2}$:Eu^{3+} phosphor with $x = 0.11$, followed by those with $x = 0.19$ and $x = 0$ (Figure 4). This strongly suggests that the displacement of the Eu^{3+} position from the centroid of [(Li, Eu)O_{12}] polyhedra contributes to the highly enhanced hypersensitive $^5D_0$–$^7F_2$ transition in Eu^{3+} when excited by near-UV light (Nakano *et al.*, 2012). The slight change of coordination environment of Eu^{3+} ion would markedly affect the *f-f* transition process, which would eventually cause an increase of emission intensity.

With $(Li_{0.967}Sm^{3+}_{0.033})(Ta_{0.89}Ti_{0.11})O_{2.978}$ ($y = 0$), the eccentricity vector $\boldsymbol{\Delta}$ is in the [001] direction with $|\boldsymbol{\Delta}| = 0.006$ nm, whereas the $\boldsymbol{\Delta}$ vector of $(Li_{0.950}Sm^{3+}_{0.033}Mg_{0.017})(Ta_{0.89}Ti_{0.11})O_{2.987}$ ($y = 0.017$) is in the opposite direction with the larger $|\boldsymbol{\Delta}|$-value of 0.046 nm (Figures 2(c) and 2(d)). Accordingly, the prominent difference between the two compounds was clarified as the degree of eccentricity along the *c*-axis of the (Li, Sm, Mg) position in [(Li, Sm, Mg)O_{12}]. The concentrations of Sm^{3+} in the Li sites of $(Li_{1-y}Mg_y)(Ta_{0.89}Ti_{0.11})O_{2.945+y/2}$:$Sm^{3+}$ are exactly the same between the two compounds with $y = 0$ and $y = 0.017$, hence the replacement of Mg for Li would mainly induce the displacement of the (Li, Sm, Mg) site along the *c*-axis, keeping both [(Li, Sm, Mg)O_{12}] and [(Ta, Ti)O_6] polyhedra nearly undistorted. Each of the PL spectra in the range

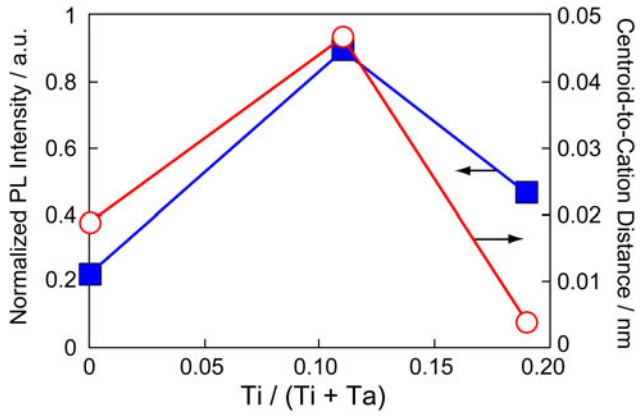

Figure 4. (Color online) Relationship between normalized photoluminescence (PL) intensity and centroid-to-cation distance (Δ-value) of [(Li, Eu)O_{12}] polyhedra with Ti/(Ti + Ta) ratio (=x) for Li$(Ta_{1-x}Ti_x)O_{3-x/2}$:Eu^{3+}. The PL intensity data are from Nakano *et al.* (2012). The Δ-value with $x = 0.11$ is from Uchida *et al.* (2013).

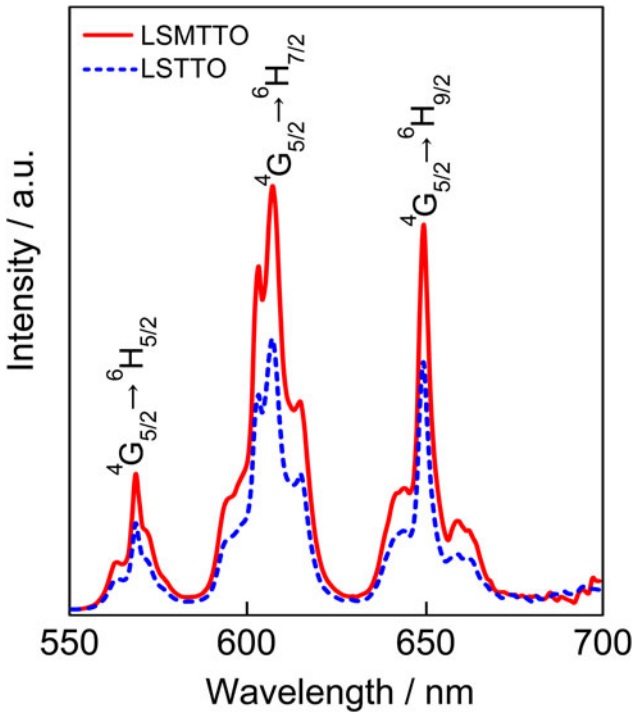

Figure 5. (Color online) Photoluminescence (PL) emission spectra of $(Li_{0.967}Sm^{3+}_{0.033})(Ta_{0.89}Ti_{0.11})O_{2.978}$ in sample LSTTO and $(Li_{0.950}Sm^{3+}_{0.033}Mg_{0.017})(Ta_{0.89}Ti_{0.11})O_{2.987}$ in sample LSMTTO, showing the higher PL intensity for the latter phosphor ($\lambda_{ex} = 410$ nm).

https://doi.org/10.1017/S0885715615000688 Published online by Cambridge University Press

550–680 nm, recorded at the excitation wavelength 410 nm, is caused by the $^4G_{5/2} \rightarrow {}^6H_J$ transitions of Sm^{3+} ion (Sakirzanovas *et al.*, 2011; Dillip *et al.*, 2013) and consists of three groups of narrow band emission in the range of 550–585 ($J = 5/2$), 585–625 ($J = 7/2$), and 630–680 ($J = 9/2$) (Figure 5). Among them, the most intense band is located at ~607 nm because of the $^4G_{5/2} \rightarrow {}^6H_{7/2}$ transition. The relevant PL intensities were ~1.6 times higher for $(Li_{0.950}Sm^{3+}{}_{0.033}Mg_{0.017})(Ta_{0.89}Ti_{0.11})O_{2.987}$ ($y = 0.017$) than for $(Li_{0.967}Sm^{3+}{}_{0.033})(Ta_{0.89}Ti_{0.11})O_{2.978}$ ($y = 0$), which strongly suggests that the displacement of the Sm^{3+} position from the centroid of [(Li, Sm, Mg)O_{12}] polyhedra contributes to the higher PL efficiency.

We have confirmed that the crystal structures of doped lithium tantalate phosphors are flexible with respect to the substitution of Eu^{3+}, Sm^{3+}, and Mg for Li and that of Ti for Ta. A more detailed discussion on the PL properties of $Li(Ta_{1-x}Ti_x)O_{3-x/2}:Eu^{3+}$ and $(Li_{1-y}Mg_y)(Ta_{0.89}Ti_{0.11})O_{2.945+y/2}:Sm^{3+}$ would be made based on the comparison among the electronic states of these compounds, which might be determined by, for example, density functional theory. The reliable atomic coordinates, which are essential for the theoretical calculations, are available at the moment for the doped lithium tantalate phosphors.

IV. CONCLUSION

We clarified the slight differences among the crystal structures of $Li(Ta_{1-x}Ti_x)O_{3-x/2}:Eu^{3+}$ ($x = 0$ and 0.19) and $(Li_{1-y}Mg_y)(Ta_{0.89}Ti_{0.11})O_{2.945+y/2}:Sm^{3+}$ ($y = 0$ and 0.017), each of which is made up of two types of polyhedra [(Li, Eu, Sm, Mg)O_{12}] and [(Ta, Ti)O_6]. The 3D EDDs determined by MPF method well supported the validity of the structural models. The substitution of Ti for Ta and that of Mg for Li displaced, respectively, the (Li, Eu) site of $Li(Ta_{1-x}Ti_x)O_{3-x/2}:Eu^{3+}$ and (Li, Sm, Mg) site of $(Li_{1-y}Mg_y)(Ta_{0.89}Ti_{0.11})O_{2.945+y/2}:Sm^{3+}$ along their *c*-axes, without changing the outer shapes of both [(Li, Eu, Sm, Mg)O_{12}] and [(Ta, Ti)O_6] polyhedra. The eccentricity of the Eu^{3+} and Sm^{3+} positions in [(Li, Eu, Sm, Mg)O_{12}] thus seems to be closely related to the PL efficiency of the doped lithium tantalate phosphors. Based on the sufficient experimental evidence for the relevant phosphors, we could be able to formulate the relationship between the magnitude of eccentricity and photoluminescence intensity.

SUPPLEMENTARY MATERIALS

For supplementary material for this article, please visit http://dx.doi.org/10.1017/S0885715615000688

ACKNOWLEDGMENT

This work was partially supported by a Grant-in-Aid for Scientific Research (c) No. 25420709 by the Japan Society for the Promotion of Science (H. N.).

Agulyanskii, A. l., Bessonova, V. A., Kuznetsov, V. Ya., and Kalinnikov, V. T. (**1986**). "Double oxide fluorides with a sodium chloride structure," Russ. J. Inorg. Chem. **31**, 1548–1549.

Balic-Zunic, T. and Vickovic, I. (**1996**). "IVTON – a program for the calculation of geometrical aspects of crystal structures and some crystal chemical applications," J. Appl. Crystallogr. **29**, 305–306.

Brindley, G. W. (**1945**). "A theory of X-ray absorption in mixed powders," Philos. Mag. **36**, 347–369.

Dillip, G. R., Kumar, P. M., Raju, B. D. P., and Dhoble, S. J. (**2013**). "Synthesis and luminescence properties of a novel $Na_6CaP_2O_9:Sm^{3+}$ phosphor," J. Lumin. **134**, 333–338.

Hsu, R., Maslen, E. N., Du Boulay, D., and Ishizawa, N. (**1997**). "Synchrotron X-ray studies of $LiNbO_3$ and $LiTaO_3$," Acta Crystallogr., Sect. B: Struct. Sci. **53**, 420–428.

Izumi, F. and Momma, K. (**2007**). "Three-dimensional visualization in powder diffraction," Solid State Phenom. **130**, 15–20.

Izumi, F., Kumazawa, S., Ikeda, T., Hu, W.-Z., Yamamoto, A., and Oikawa, K. (**2001**). "MEM-based structure-refinement system REMEDY and its applications," Mater. Sci. Forum **378–381**, 59–64.

Krylov, E. I. and Strelina, M. M. (**1963**). "Orthotantalates of lanthanum, samarium, and europium," Russ. J. Inorg. Chem. **8**, 1180–1182.

Leonidov, I. A., Leonidova, O. N., Perelyaeva, L. A., Samigullina, R. F., Kovyazina, S. A., and Patrakeev, M. V. (**2003**). "Structure, ionic conduction, and phase transformations in lithium titanate $Li_4Ti_5O_{12}$," Phys. Solid State **45**, 2183–2188.

Makovicky, E. and Balic-Zunic, T. (**1998**). "New measure of distortion for coordination polyhedra," Acta Crystallogr. Sect. B: Struct. Sci. **B54**, 766–773.

Momma, K. and Izumi, F. (**2011**). "VESTA 3 for three-dimensional visualization of crystal, volumetric and morphology data," J. Appl. Crystallogr. **44**, 1272–1276.

Momma, K., Ikeda, T., Belik, A. A., and Izumi, F. (**2013**). "Dysnomia, a computer program for maximum-entropy method (MEM) analysis and its performance in the MEM-based pattern fitting," Powder Diffr. **28**, 184–193.

Nakano, H., Ozono, K., Hayashi, H., and Fujihara, S. (**2012**). "Synthesis and luminescent properties of a new Eu^{3+}-Doped $Li_{1+x}(Ta_{1-z}Nb_z)_{1-x}Ti_xO_3$ red phosphor," J. Am. Ceram. Soc. **95**, 2795–2797.

Nakano, H., Suehiro, S., Furuya, S., Hayashi, H., and Fujihara, S. (**2013**). "Synthesis of new RE^{3+} doped $Li_{1+x}Ta_{1-x}Ti_xO_3$ (RE: Eu, Sm, Er, Tm, and Dy) phosphors with various emission colors," Materials **6**, 2768–2776.

Rietveld, H. M. (**1967**). "Line profiles of neutron powder-diffraction peaks for structure refinement," Acta Crystallogr. **22**, 151–152.

Sakirzanovas, S., Katelnikovas, A., Bettentrup, H., Kareiva, A., and Jüstel, T. (**2011**). "Synthesis and photoluminescence properties of Sm^{3+}-doped $LaMgB_5O_{10}$ and $GdMgB_5O_{10}$," J. Lumin. **131**, 1525–1529.

Takata, M., Nishibori, E., and Sakata, M. (**2001**). "Charge density studies utilizing powder diffraction and MEM. Exploring of high Tc superconductors, C60 superconductors and manganites," Z. Kristallogr. **216**, 71–86.

Uchida, T., Suehiro, S., Asaka, T., Nakano, H., and Fukuda, K. (**2013**). "Syntheses and crystal structures of $Li(Ta_{0.89}Ti_{0.11})O_{2.945}$ and $(Li_{0.977}Eu_{0.023})(Ta_{0.89}Ti_{0.11})O_{2.968}$," Powder Diffr. **28**, 178–183.

Young, R. A. (**1993**). "Introduction to the Rietveld method," in *The Rietveld Method*, edited by R. A. Young (Oxford University Press, Oxford, U.K.), pp. 1–38.